Tissue alignment enhances remodeling potential of tendon-derived cells - Lessons from a novel microtissue model of tendon scarring

Foolen, Jasper ; Wunderli, Stefania L ; Loerakker, Sandra ; Snedeker, Jess G

Abstract: Tendinopathy is a widespread and unresolved clinical challenge, in which associated pain and hampered mobility present a major cause for work-related disability. Tendinopathy associates with a change from a healthy tissue with aligned extracellular matrix (ECM) and highly polarized cells that are connected head-to-tail, towards a diseased tissue with a disorganized ECM and randomly distributed cells, scar-like features that are commonly attributed to poor innate regenerative capacity of the tissue. A fundamental clinical dilemma with this scarring process is whether treatment strategies should focus on healing the affected (disorganized) tissue or strengthen the remaining healthy (anisotropic) tissue. The question was thus asked whether the intrinsic remodeling capacity of tendon-derived cells depends on the organization of the 3D extracellular matrix (isotropic vs anisotropic). Progress in this field is hampered by the lack of suitable in vitro tissue platforms. We aimed at filling this critical gap by creating and exploiting a next generation tissue platform that mimics aspects of the tendon scarring process; cellular response to a gradient in tissue organization from isotropic (scarred/non-aligned) to highly anisotropic (unscarred/aligned) was studied, as was a transient change from isotropic towards highly anisotropic. Strikingly, cells residing in an 'unscarred' anisotropic tissue indicated superior remodeling capacity (increased gene expression levels of collagen, matrix metalloproteinases MMPs, tissue inhibitors of MMPs), when compared to their 'scarred' isotropic counterparts. A numerical model then supported the hypothesis that cellular remodeling capacity may correlate to cellular alignment strength. This in turn may have improved cellular communication, and could thus relate to the more pronounced connexin43 gap junctions observed in anisotropic tissues. In conclusion, increased tissue anisotropy was observed to enhance the cellular potential for functional remodeling of the matrix. This may explain the poor regenerative capacity of tenocytes in chronic tendinopathy, where the pathological process has resulted in ECM disorganization. Additionally, it lends support to treatment strategies that focus on strengthening the remaining healthy tissue, rather than regenerating scarred tissue.

DOI: https://doi.org/10.1016/j.matbio.2017.06.002

Originally published at:
Foolen, Jasper; Wunderli, Stefania L; Loerakker, Sandra; Snedeker, Jess G (2018). Tissue alignment enhances remodeling potential of tendon-derived cells - Lessons from a novel microtissue model of tendon scarring. Matrix Biology, 65:14-29.
DOI: https://doi.org/10.1016/j.matbio.2017.06.002

Tissue alignment enhances remodeling potential of tendon-derived cells - Lessons from a novel microtissue model of tendon scarring

Jasper Foolen [a,b,c], Stefania L. Wunderli [a,b], Sandra Loerakker [c] and Jess G. Snedeker [a,b]

a - Department of Orthopaedics, *University Hospital Balgrist, Lengghalde 5, CH-8008 Zurich, Switzerland*
b - Institute for Biomechanics, *ETH Zurich, Lengghalde 5, CH-8008 Zurich, Switzerland*
c - Department of Biomedical Engineering, *Eindhoven University of Technology, Eindhoven, The Netherlands*

Correspondence to Jess G. Snedeker: *Department of Orthopaedics, University Hospital Balgrist, Lengghalde 5, CH-8008 Zurich, Switzerland. jess.snedeker@hest.ethz.ch*
http://dx.doi.org/10.1016/j.matbio.2017.06.002

Abstract

Tendinopathy is a widespread and unresolved clinical challenge, in which associated pain and hampered mobility present a major cause for work-related disability. Tendinopathy associates with a change from a healthy tissue with aligned extracellular matrix (ECM) and highly polarized cells that are connected head-to-tail, towards a diseased tissue with a disorganized ECM and randomly distributed cells, scar-like features that are commonly attributed to poor innate regenerative capacity of the tissue. A fundamental clinical dilemma with this scarring process is whether treatment strategies should focus on healing the affected (disorganized) tissue or strengthen the remaining healthy (anisotropic) tissue. The question was thus asked whether the intrinsic remodeling capacity of tendon-derived cells depends on the organization of the 3D extracellular matrix (isotropic vs anisotropic). Progress in this field is hampered by the lack of suitable in vitro tissue platforms. We aimed at filling this critical gap by creating and exploiting a next generation tissue platform that mimics aspects of the tendon scarring process; cellular response to a gradient in tissue organization from isotropic (scarred/non-aligned) to highly anisotropic (unscarred/aligned) was studied, as was a transient change from isotropic towards highly anisotropic. Strikingly, cells residing in an 'unscarred' anisotropic tissue indicated superior remodeling capacity (increased gene expression levels of collagen, matrix metalloproteinases MMPs, tissue inhibitors of MMPs), when compared to their 'scarred' isotropic counterparts. A numerical model then supported the hypothesis that cellular remodeling capacity may correlate to cellular alignment strength. This in turn may have improved cellular communication, and could thus relate to the more pronounced connexin43 gap junctions observed in anisotropic tissues. In conclusion, increased tissue anisotropy was observed to enhance the cellular potential for functional remodeling of the matrix. This may explain the poor regenerative capacity of tenocytes in chronic tendinopathy, where the pathological process has resulted in ECM disorganization. Additionally, it lends support to treatment strategies that focus on strengthening the remaining healthy tissue, rather than regenerating scarred tissue.

Introduction

Tendon and ligament injuries account for 30% of all musculoskeletal consultations [1], presenting a high clinical demand with approximately 4 million new (reported worldwide) incidents annually [2]. These cases are attributed to acute damage (tears or cuts) as well as fatigue damage (chronic loading) [3–6]. Not surprisingly, tendinopathy is a frequent cause (30–50%) of injuries related to sports and other rigorous physical activities [4,7–9], which together with an aging yet increasingly active population gives rise to increasing prevalence [4,10,11]. Surgical interventions that aim at reconstructing tendons using grafts in

severe cases, lack good clinical outcome because of various drawbacks, e.g. donor site morbidity [12,13], immunological rejection [14] and poor graft integration [15,16]. These drawbacks can cause re-tears in 35 to 95% of the cases [17,18]. The poor healing capacity due to limited cell numbers with low metabolism and poor blood supply [7,19,20] also limits the progress made in the treatment of tendinopathy over the past decades [21].

Tendon tissue repair and tendinopathy are both often characterized by the formation of a fibrotic scar [22–24], with potentially accompanying pain, hampered mobility, and work-related disability [25–27]. This scarring process is characterized by a deviation from highly organized (anisotropic) tissue towards a more disorganized (isotropic) tissue [28], with impaired mechanical strength [25–27]. A known compensation mechanism for the decreased mechanical strength is an increase in tissue cross-sectional area [29,30]. This can explain the positive effect of exercise on treating tendinopathy [31–36], although a recent review states that such clinical interventions do not aid in transforming disorganized tissue subregions back to their original anisotropy [37]. The beneficial effect of such treatment could thus be a result of strengthening the tissue as a whole, i.e. the remaining healthy tissue but not the restructuring of the affected isotropic region, as recently suggested recently [30,38]. Deeper insight is thus required to unravel the regenerative potential of cells that reside in a scarred isotropic region, in comparison to cells that reside in anisotropic regions. Discrepancies could provide an underlying mechanism for the poor regenerative capacity of isotropic scarred tissue.

Variations in the aspect ratio of cellular morphology has a large effect on cell behavior [39–41]. For healthy tendons, the strong anisotropic organization results in high aspect ratios of the cells that are longitudinally oriented. This longitudinal orientation may originate from the particular size range (20–200 μm) of the tendon subunits, i.e. the (sub)fascicles [42]. This suggestion follows from a study in which conflicting cues for steering cellular orientation were presented, i.e. width of a cell-adhesive macropattern vs. perpendicular micropatterns. Only when the width of the cell-adhesive macropattern stayed within the range of a fascicle (250 μm), the cellular F-actin respected the macropattern [42]. Such cues resulting in alignment of tendon-derived cells in turn affect their intrinsic behavior. Porcine tenocytes cultured on smooth silicon membranes showed a decrease in gene expression of the tendon marker tenomodulin and of collagen I, when compared to anisotropic microgrooved membranes [43]. Similar trends were observed for human fetal tendon stem cells seeded on aligned or random PLLA scaffolds. On aligned scaffolds, a higher expressions of tendon specific markers (Eya2 and Scleraxis), and equally important a suppression of osteogenic differentiation (RUNX2 and ALP gene expression & ALP and Alizarin Red positive cells) was detected [44,45]. Additionally, thicker collagen fibers were formed in anisotropic scaffolds with improved histological appearance [45]. Exposing tendon-derived cells to anisotropic substrates, when compared to isotropic substrates, is thus beneficial for tenogenic gene expression, however this does not reveal whether the functional remodeling capacity of tendon-derived cells depends on the organization of the 3D environment (isotropic vs anisotropic).

We therefore asked if the remodeling capacity of tendon-derived cells depends on the degree of tissue anisotropy. In an attempt to answer this question, an experimental-numerical approach was adopted. Experimentally, tendon-derived cells were embedded in 3D tissue model systems (Fig. 1), varying from completely anisotropic ('unscarred', tissues anchored to 2 opposing posts) to isotropic ('scarred', tissues anchored to 12 posts in a square setup). Gene expression patterns between the different setups were compared for tenogenic stability, matrix composition, cell-cell contact and remodeling capacity. Subsequently, a numerical model was exploited to quantify the potential underlying mechanism of cellular alignment in the different model systems to the measured anisotropy-dependent gene expression profiles. We hereby aimed at understanding the fundamental potential of tendon functional remodeling as a function of the scarring process, which can potentially explain the lack of adequate healing of tendinopathy-affected tissue.

Results

Tuning boundary constraints directs cellular organization

Tissue platforms were designed (Fig. 1) that mimic tendon/ligament 'unscarred' tissue (2 posts) with strong cellular anisotropy, progressively changing towards 'scarred' (12 posts) with an isotropic cellular orientation, as assessed by staining of the F-actin cytoskeleton at day 4 (Fig. 2A) and day 7 (Fig. 2B) after gel seeding. Especially at day 7 after seeding, qualitative assessment of nuclear shape also showed a gradient between tissue platforms, from polarized in anisotropic tissue (2 posts) towards more round in isotropic tissue (12 posts).

High tissue anisotropy enhances matrix remodeling potential

Next, the designed tissue platforms were exploited to detect organization-related gene expression changes using quantitative RT-PCR, with a focus on tenogenic stability, cellular communication and

Please cite this article as: J. Foolen, et al., Tissue alignment enhances remodeling potential of tendon-derived cells - Lessons from a novel microtissue model of tendon scarri..., Matrix Biol (2017), http://dx.doi.org/10.1016/j.matbio.2017.06.002

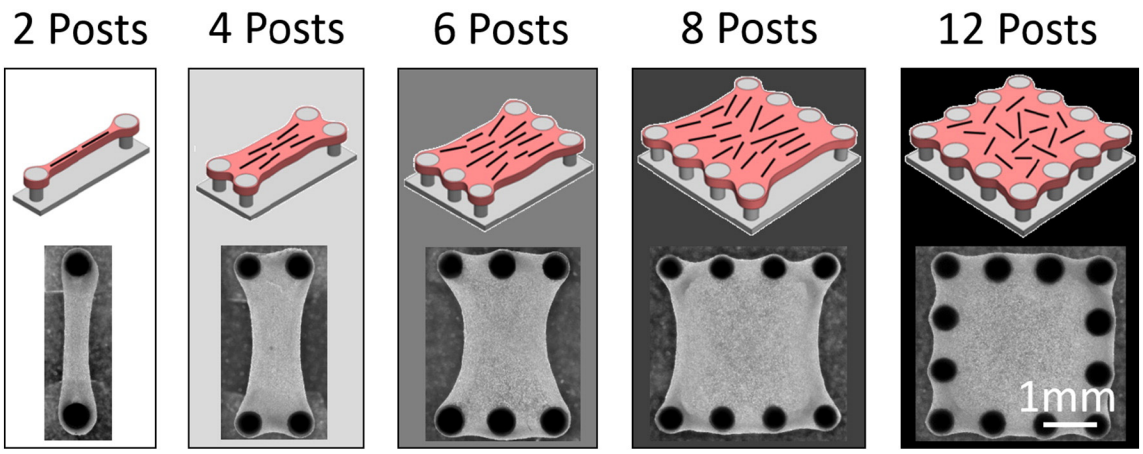

Fig. 1. Tissue platform that ranges from highly anisotropic (2 posts) towards highly isotropic (12 posts. The platform is designed to mimic 'unscarred' tendon tissue (2 posts, highly anisotropic, towards progressively more 'diseased and scarred' tendon tissue (12 posts, highly isotropic).

matrix turnover. For both time points, increasing trends in expression of matrix remodeling genes (MMPs and TIMPs, Fig. 3A) were observed with increasing tissue anisotropy, with the exception of MMP3. Increasing trends were also observed for gene expression values related to collagen production (Col I and III, Fig. 3B), when moving from isotropic tissue (12 posts) towards anisotropic tissue (2 posts), although only at day 4. These trends for MMPs, TIMPs and collagen are indicative for a decreased cell-derived remodeling potential when populating matrices that are progressively more isotropic.

Connexins are gap junctions that serve as communication portals, primarily via transportation of molecules and ions. In tendon, connexin 26, 32 and 43 are detected, where connexin 43 (Cx43) is found predominantly between cells that are connected head-to-tail and thus in the longitudinal direction of the tissue [46,47]. Cx43 expression was shown to increase with increasing anisotropy, most notably at day 7, which is indicative for enhanced functional cellular communication in anisotropic compared to isotropic tissues. Connexin 26 and 32 were also measured in the current study, but their C_T values sporadically crossed the detection limit and were therefore excluded from the presented data.

Decorin (Dcn) plays a dominant role in collagen fibrillogenesis and establishing the high degree of tissue anisotropy in healthy tendon [48], and a stronger response was therefore expected for anisotropic tissue. However, a moderate increasing trend was observed for decorin (Dcn), from isotropic to anisotropic tissues and only at day 4, without significant differences between the groups.

Tenogenic expression and differentiation was assessed by measuring tendon-related genes (scleraxis: Scx, tenomodulin: Tnd, mohawk: Mkx) and genes related to myofibroblastic differentiation (alpha smooth muscle actin: αSMA and connective tissue growth factor: CTGF). Trends were visible for scleraxis and mohawk (day 4 and 7, Fig. 3A), with the highest expression values for the anisotropic (2 posts) setup, gradually decreasing towards the isotropic (12 posts) setup. Due to the higher standard deviations associated with αSMA and CTGF expression, trends for these genes are unlikely to be meaningful. Although without showing a clear gradient, tenomodulin at day 7 was lowest in the anisotropic tissue. This is surprising since scleraxis is an early tendon marker upstream of tenomodulin [49], and a correlation between the two genes was therefore expected.

Mean cellular alignment strength may be a measure for cellular remodeling potential

Measured gene expression levels, as described before (Fig. 3), are analyzed in the context of tissue anisotropy (Fig. 2). A complication however is that gene expression levels were obtained from the complete tissue whereas cellular anisotropy (F-actin orientation) was visualized only in the tissue core (Fig. 2). Recent work showed that in close vicinity of constraining posts, cells display strong anisotropy [50]. It thus is feasible that more locations with a strong alignment can be found for the 12 posts setup, compared to the 8 posts setup. This could have important implications, since decreasing trends in gene expression were frequently observed from 2 posts to 8 posts, where this trend increased again towards 12 posts (at day 4: Cx43 & Timp1, at day 7: Scx, Mkx, Col III, Cx43, MMP1, 2, 3, 9, 13, 14, Timp1 & 2). We set out to evaluate whether this deviation in gene expression levels in the 12 posts setup can be attributed to differences in the degree of overall tissue alignment strength. Since the tissues are too large to be fully imaged for cellular alignment, a previously

Please cite this article as: J. Foolen, et al., Tissue alignment enhances remodeling potential of tendon-derived cells - Lessons from a novel microtissue model of tendon scarri..., Matrix Biol (2017), http://dx.doi.org/10.1016/j.matbio.2017.06.002

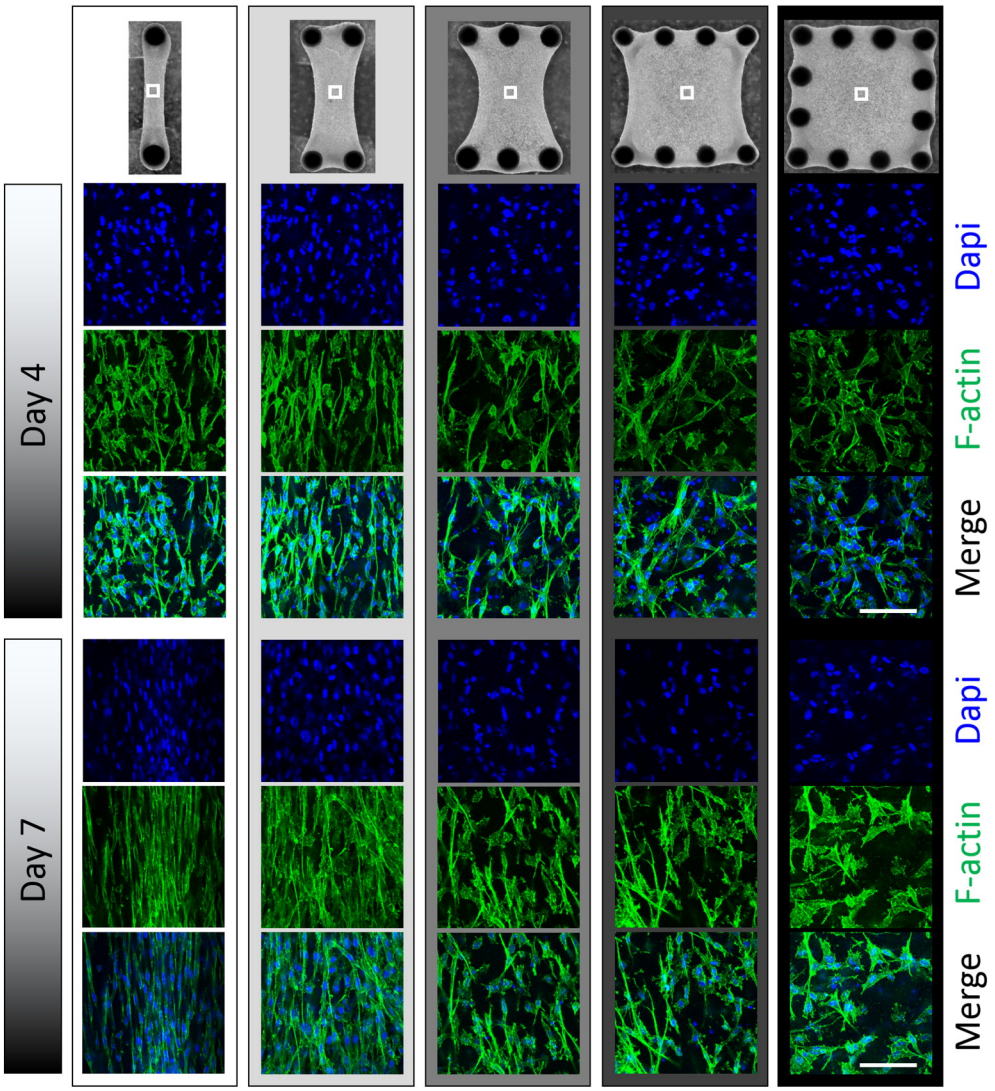

Fig. 2. Different tissue setups result in a gradient of intracellular stress fiber (F-actin) orientation, ranging from highly anisotropic (2 posts), gradually towards isotropic (12 posts), both at day 4 and day 7, where alignment strength appears to further increase over time for anisotropic tissues. Images are representative for the stress fiber organization in the tissue core, as indicated by the white square. All scale bars represent 100 μm.

validated numerical approach was adopted to assess location-specific alignment strength and subsequently translate these data into alignment strength parameters, representative for the tissue as a whole.

The computational framework uses a continuum mechanics approach to predict the remodeling of actin stress fibers in response to mechanical cues, where cell-seeded gels are modeled as mixtures of actin stress fibers, collagen fibers, and isotropic cell and tissue constituents [50–52]. Using this numerical model, the local predicted cell orientation (represented by stress fiber alignment) was observed to correlate well with overall collagen alignment of the polarized light microscopy images for all tissue setups on a qualitative level (Fig. 4A & B). Additionally, the predicted strength of the stress fiber alignment in the core of the tissue was found to decrease with decreasing anisotropy, in line with the observed alignment of intracellular stress fibers in the experimental setups (Fig. 2, F-actin).

In order to compare whole tissue alignment and gene expression levels, the average alignment strength of the whole tissue (Mean Strength A) was determined for each of the modeled setups (see materials and methods for details). This alignment index appeared to decrease monotonically with the number of posts in the setups (Fig. 4C, Mean Strength A), and hence does not provide a potential explanation for the observed trends in gene expression levels in the experiments. Interestingly, however, when local gene expression levels were hypothesized to depend exponentially on the local alignment strength in the

Please cite this article as: J. Foolen, et al., Tissue alignment enhances remodeling potential of tendon-derived cells - Lessons from a novel microtissue model of tendon scarri..., Matrix Biol (2017), http://dx.doi.org/10.1016/j.matbio.2017.06.002

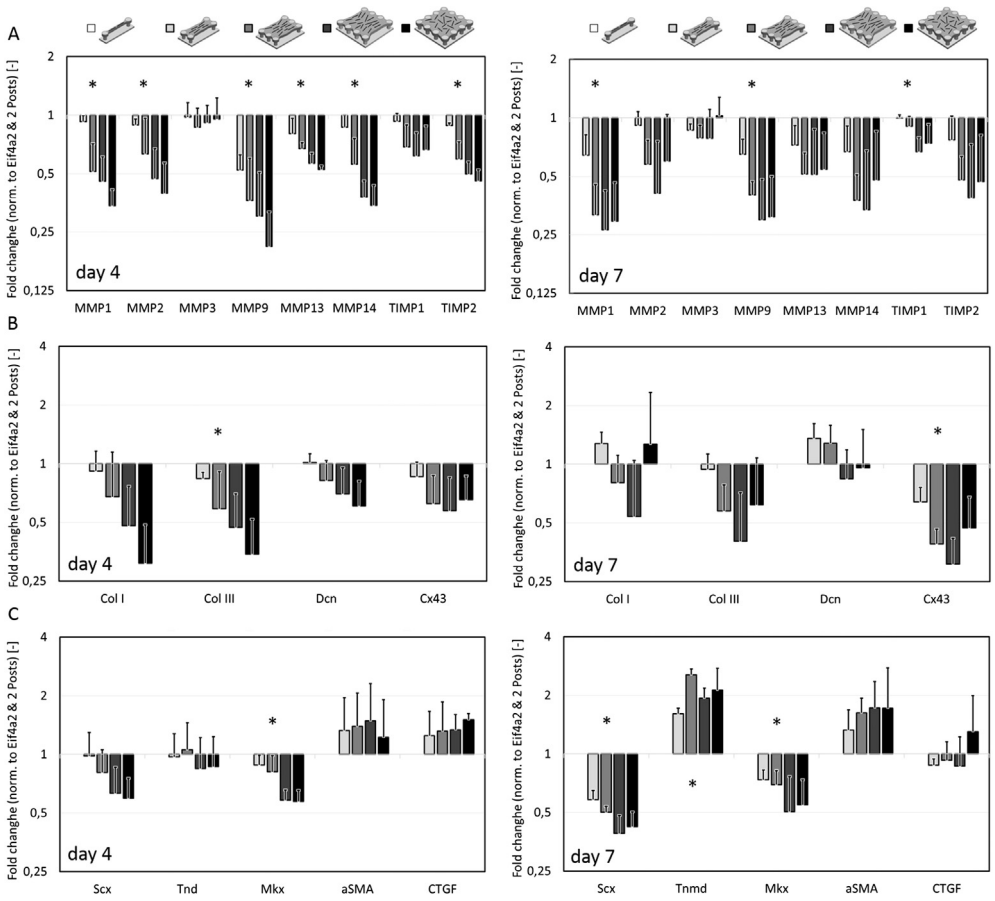

Fig. 3. Increased tissue anisotropy results in enhanced cellular remodeling potential, as visible from the gradual decrease in gene expression towards the isotropic (12 post) setup for many MMPs, TIMPs & Collagen. Increased anisotropy also appears to be beneficial for cellular communication (connexin43) and tenogenic expression (Scx and Mkx, but not Tnd). An * represents a significant difference between groups (one-way ANOVA, no post-hoc test). For all experiments, $n = 3$.

model, then the total predicted 'gene expression' of each tissue (corrected for differences in volume) showed similar trends as observed experimentally, i.e. a monotonic decrease from 2 to 8 posts and a subsequent increase in the 12 posts setup (Fig. 4C, Mean Strength B). Although it should be noted that the specific exponential function used in the model just serves as an example, this result clearly shows that a nonlinear dependence of gene expression on local cell alignment may explain the observed experimental trends in overall gene expression. Taken together, our numerical framework suggests that the observed changes in gene expression between the different setups may be attributed to differences in overall cell alignment in combination with a nonlinear dependence of local gene expression on local cell alignment.

Cellular anisotropy potentially improves cellular communication

Cellular alignment strength may affect cellular communication, in analogy to healthy tendon where connexin43 links head-to-tail arranged cells [46,47], and could be an underlying cause for the observed gradients in gene expression levels. Therefore, gap junction protein connexin 43, shown to be significantly different between the different platforms (Fig. 3, Cx43 at day 7), was fluorescently labeled in all tissue setups at day 7 (Fig. 5, left column). Connexin 43 appeared to be more punctate in the anisotropic tissue to become progressively more cytoplasmic towards the isotropic tissue. This may indicate a tendency for improved cellular communication with increasing tissue anisotropy, which may in turn explain the observed increases in gene expression levels.

Enhanced remodeling capacity, as observed for anisotropic tissues compared to isotropic tissues, can be a sign of myofibroblastic differentiation of tendon-derived cells. Even though αSMA and CTGF gene expression levels were not significantly different between groups (Fig. 3), the protein may vary between groups on a functional level. Cells were thus fluorescently labeled for αSMA in all setups (Fig. 5, right column). αSMA appears to become more locally expressed when moving towards isotropic tissue. However, a possible implication of this should

Please cite this article as: J. Foolen, et al., Tissue alignment enhances remodeling potential of tendon-derived cells - Lessons from a novel microtissue model of tendon scarri..., Matrix Biol (2017), http://dx.doi.org/10.1016/j.matbio.2017.06.002

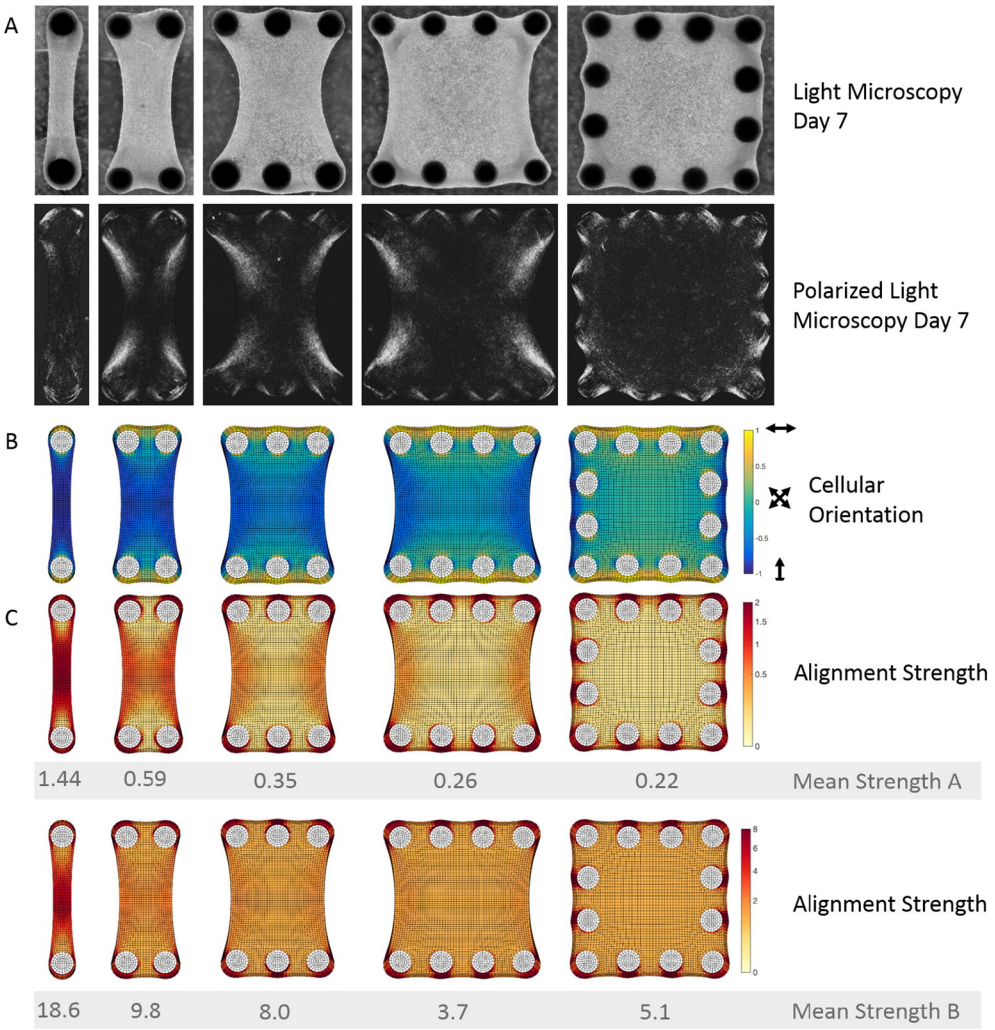

Fig. 4. Cellular alignment strength may be a potential driver for remodeling-related gene expression. Fig. 4A: Representative light microscopy images (top row) and polarized light microscopy images (bottom row) of the different platforms. Fig. 4B & C: good agreement between the global orientation and alignment strength is obtained between the model and the polarized light images. Additionally, the center of the tissue shifts from strongly anisotropic (2 posts) gradually towards isotropic (12 posts), in agreement with stress fiber orientation, as shown in Fig. 2. Mean Strength A and B represent the average of alignment strength over all voxels in the model, where in A, a linear weight is given, and in B alignment strength exponentially contributes to the Mean Strength value. It is hereby hypothesized that alignment strength may be a predictor for expression values of several genes, as shown in Fig. 3.

be carefully approached, especially since co-localization with F-actin was not observed.

Tissue perturbation results in rapid cellular reorganization

One drawback of the used tissue platforms is the necessity to compare cells residing in tissues of different morphology (Fig. 1). To confirm a dependency of tissue anisotropy on gene regulation, the model system was slightly adapted to enable the measurement of transient changes in cellular alignment, i.e. from predominantly isotropic gradually towards anisotropic (Fig. 6). Tissues that were cultured while retaining their geometry (unperturbed), displayed a random organization of the F-actin cytoskeleton. On the contrary, tissues from which perpendicular boundary constraints were removed (perturbed), remodeled towards anisotropic tissues with corresponding F-actin orientation. A platform was thus developed in which cellular behavior to changing tissue anisotropy can be measured.

Cellular anisotropy appears to provoke a positive remodeling response

The platform (Fig. 6) was subsequently exploited to assess changes on the gene expression level for maintenance versus change in tissue anisotropy.

Please cite this article as: J. Foolen, et al., Tissue alignment enhances remodeling potential of tendon-derived cells - Lessons from a novel microtissue model of tendon scarri..., Matrix Biol (2017), http://dx.doi.org/10.1016/j.matbio.2017.06.002

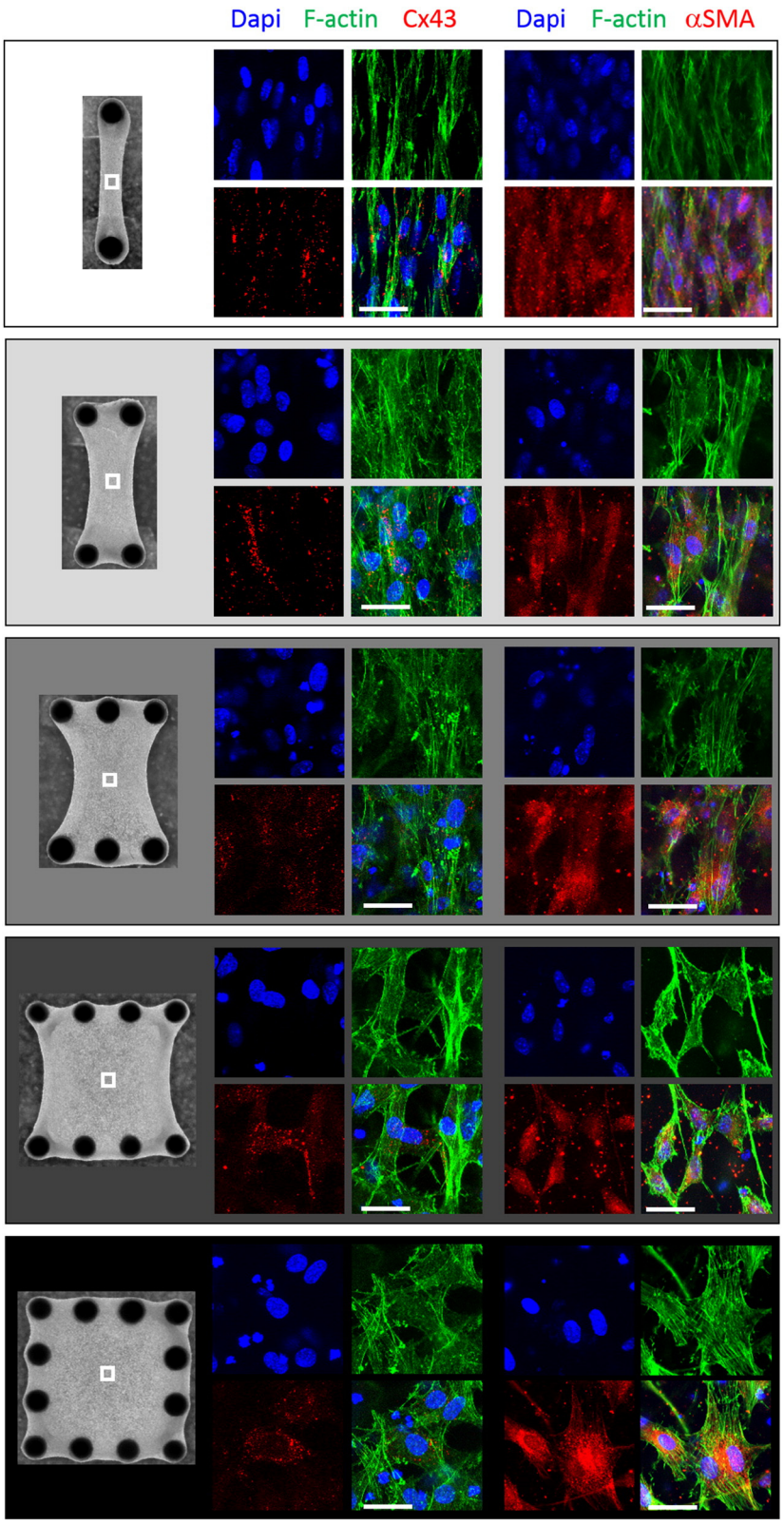

Fig. 5. Connexin43 staining (Cx43, left column) appeared to change from more cytoplasmic for isotropic tissues towards more punctate for anisotropic tissues, indicative for improved cellular communication. For alpha smooth muscle actin (αSMA, right column), co-localization with F-actin was not observed, however the protein appeared to become more locally expressed moving towards isotropic tissues. Images are taken at day 7 of culturing. All scale bars represent 25 μm.

Gene expression measurements were performed with quantitative RT-PCR at day 2 (day 4 after seeding) and 5 (day 7 after seeding) after tissue perturbation (tissue perturbation was performed at day 2 after seeding). A comparison was made between perturbed and unperturbed tissues at both time points,

Please cite this article as: J. Foolen, et al., Tissue alignment enhances remodeling potential of tendon-derived cells - Lessons from a novel microtissue model of tendon scarri..., Matrix Biol (2017), http://dx.doi.org/10.1016/j.matbio.2017.06.002

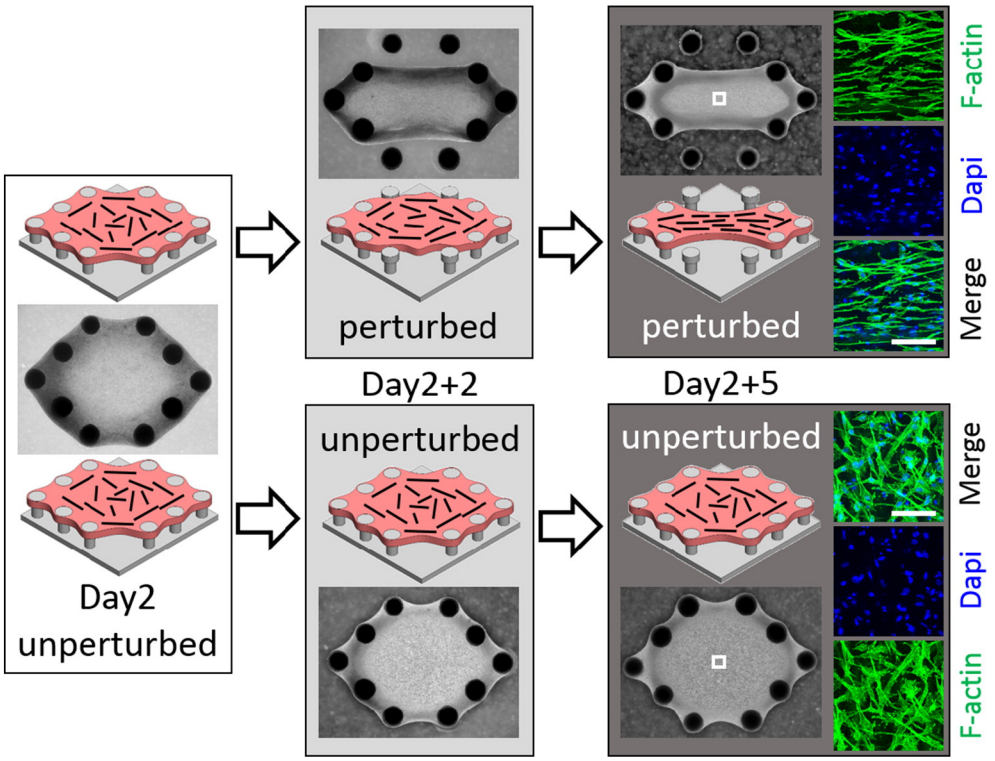

Fig. 6. Tissue remodeling platform, inducing a transient change in cellular alignment, as shown on the right. Tissues that were cultured, while retaining their geometry, showed a random organization of the F-actin cytoskeleton, compared to tissues that started with the same initial geometry but remodeled into a tissue with a highly aligned F-actin orientation after removing perpendicular boundary constraints. Fluorescent images originate from the white box in the light microscopy images. Scale bar represents 100 μm.

normalized against the expression levels at day 2 (Fig. 7). At day 5 after perturbation (Day 2 + 5), perturbed tissues with enhanced cellular alignment had higher expression levels of scleraxis, mohawk, collagen I and III, connexin43, MMPs and TIMPs, when compared to unperturbed tissues. Trends were thus consistent with the data presented in Fig. 3. At day 2 after perturbation (Day 2 + 2), clear trends were not observed and this time point may have been too early for gene expression profiles to have already changed.

Discussion

Tendinopathy and connective tissue fibrosis are widespread and clinically unresolved challenges due to poor innate regenerative capacity and ineffective treatment strategies, that often involve emergence of fibrotic scar tissue [22–24]. The scarring process is a limiting factor for the healing outcome, since it associates with a progressive disorganization of the tissue (ECM and cells) [28] with impaired mechanical strength [25–27]. However, it remains unclear how this altered organization in turn directly affects cellular behavior. Are cells stimulated to initiate a healing process or do they lose regenerative capacity when exposed to a disorganized environment? This work addressed the question whether the matrix remodeling capacity of tendon-derived cells depends on the organization of the 3D environment (isotropic vs. anisotropic). This question was tackled by designing and exploiting a tissue platform that aimed at mimicking the change in matrix organization over the entire disease course, i.e. from 'unscarred' anisotropic towards 'scarred' isotropic. Strikingly, the gradient in enhanced tissue anisotropy between the platforms positively correlated with a gradient in matrix turnover capacity (Collagen, MMPs and TIMPs) and cellular communication (connexin 43). Absolute fold changes in gene expression levels were however modest. Exploitation of a numerical model then revealed that cellular alignment strength correlates with the measured gene expression values, when assuming that local alignment can affect gene expression levels exponentially. These findings may suggest that cells exposed to a progressively disorganized niche, lose their capacity for functional repair. Clinical work and animal studies have shown that healing of affected tendon tissue rarely, if ever, regains the native structure, which is the case for tendinopathy [29,53–56], but also for autografts used in ACL

Please cite this article as: J. Foolen, et al., Tissue alignment enhances remodeling potential of tendon-derived cells - Lessons from a novel microtissue model of tendon scarri..., Matrix Biol (2017), http://dx.doi.org/10.1016/j.matbio.2017.06.002

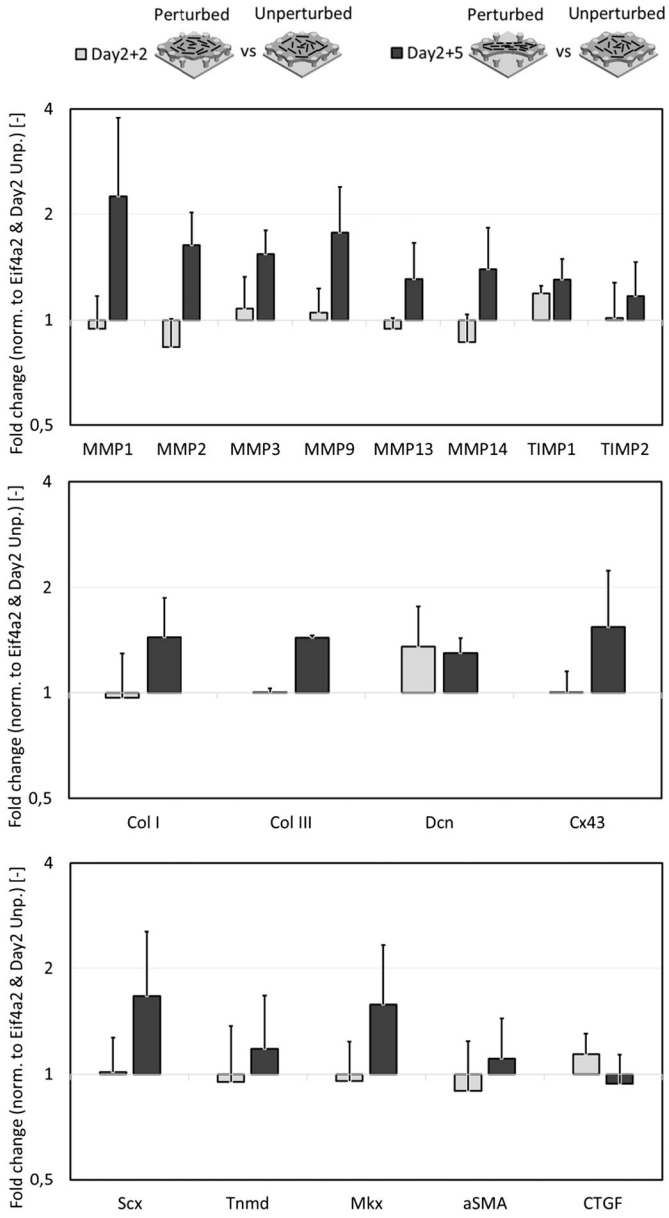

Fig. 7. A change in tissue organization from isotropic towards highly anisotropic resulted in a trend suggesting an increased remodeling potential (MMPs, TIMPs & Collagen), increased potential for cellular communication (Cx43) and increased tenogenic expression (Scx & Mkx) at day 5 after perturbation. These trends corroborate with data shown in Fig. 3. Values are normalized against the housekeeping gene Eif4a2 and unperturbed tissues at day 2. For all experiments, $n = 3$.

replacement that undergo ligamentization [57]. Future work should aim at assessing whether our finding that cells in a disorganized ECM have a diminished capacity for remodeling and thus possibly diminished healing potential, relates to such clinical implications. This could give further insight in the validity of the metaphor as stated by Cook et al. [38]: "*treat the doughnut (area of aligned fibrillar structure), not the hole (area of disorganisation)*".

The most striking finding in this paper was the gradual increase in remodeling capacity (MMPs, TIMPs and collagen) when cells were exposed to an environment that increased in anisotropy. On the basis of strong visual evidence of the formed ECM (Fig. 6), it is proposed that the elevated matrix remodeling gene activity with increased tissue anisotropy relates to an improved functional remodeling response and not a degenerative response. Healthy tendon contains high amounts of collagen type I and low amounts of type III collagen [58], whereas tendinopathy is characterized by increased production of type III collagen and higher type III/I collagen ratios [58–63]. Since an increased expression of type III collagen in anisotropic tissues, compared to isotropic tissues, is only observed at day 4, it seems unlikely to be associated with a pathological response. A similar difficulty associates with the expression of MMPs and TIMPs, since the balance between the amount of active MMPs and TIMPs is determinant for whether a net matrix synthesis or catabolism occurs [3,64–71]. Their roles are thus highly contextual, both spatially and temporally [68–70]. Nevertheless, healing rat

Please cite this article as: J. Foolen, et al., Tissue alignment enhances remodeling potential of tendon-derived cells - Lessons from a novel microtissue model of tendon scarri..., Matrix Biol (2017), http://dx.doi.org/10.1016/j.matbio.2017.06.002

Achilles tendons mechanically weakened when treated with an MMP-inhibitor [72]. Notably, MMP3, which is found to be upregulated [73–77] or downregulated [70] in pathological tendon, is the only MMP that was not sensitive to changes in tissue anisotropy – perhaps indicating a unique functional role for this MMP in tendon.

One of the factors that remains to be resolved is the driving force for the observed changes in gene expression with changing tissue organization. An attempt was made to use cellular polarity, i.e. the degree of anisotropy of the intracellular stress fiber network, as the driving force by exploiting a numerical model. As a consequence of such polarity, head-to-tail cell-cell contact and communication could be improved, which is the hallmark of healthy tendon tissue [78]. Fluorescent labeling of connexin 43 then showed a more punctate appearance in the anisotropic tissues, becoming more cytoplasmic towards the isotropic tissues, which may have been an indicator for improved communication. However, a limitation to this study is that an increase in cell density from the 2 posts to the 12 posts platform, apart from enhanced cellular alignment, can also affect the expression of connexin, i.e. a correlation between connexin 43 and 32 expression and increased cell density was previously observed for in equine digital flexor tendons [79]. Another limitation is that the rtPCR data are inherently flawed because cellular alignment varies within a tissue and analyses are performed on whole tissues. We chose to still perform PCR on whole tissues and not biopsied core tissues, as this biopsying would introduce bias due to the experimental challenge of performing this in a reproducible and consistent way (the largest tissues are 3x3mm only). Instead, we aimed at quantifying the effect of alignment variations using a numerical model. The model indicated that cellular alignment near posts is indeed stronger and thus diminishes the gradients observed for gene expression changes with platform setup, as observed using rtPCR. Future support will be gained by performing in situ hybridization studies and quantification on the protein level using western blotting.

Tissue anisotropy is one of the unique features of tendon [80], and perhaps not surprisingly strong anisotropy has been found beneficial for tenogenic expression [43–45] and stem cell differentiation towards the tenogenic lineage [65,81–83]. When cultured on aligned scaffolds, tendon-derived cells displayed superior expression of the tendon marker scleraxis, compared to randomly organized substrates, and equally important a suppression of osteogenic differentiation [44]. Also when implanted in Achilles tendon defects, aligned scaffolds compared to random scaffolds showed improved histological appearance of collagen I, and increased gene expression levels of scleraxis at 2 and 8 weeks and tenomodulin at 8 weeks post-surgery [45]. Porcine tenocytes cultured on anisotropic microgrooved membranes showed increased gene expression of the tendon marker tenomodulin and of collagen I, when compared to smooth silicon membranes [43]. Results for scleraxis and collagen I thus agree with the current study, of which gene expression was observed to gradually increase with increasing anisotropy. Also in agreement with these studies, measured differences in gene expression level between isotropic and anisotropic substrates were in the same range of the current study. Contrary to previous work, tenomodulin was lowest in tissues with the highest anisotropy, even though not showing a gradient. This is somewhat surprising since scleraxis, which in the current study did display a gradual increase in expression with increasing anisotropy, is an early tendon marker upstream of tenomodulin [49]. We thus anticipated similar trends of tenomodulin and scleraxis, although this expected co-regulation was not observed. Despite changes in tenogenic expression (scleraxis, tenomodulin and mohawk), our tissue platform was not sufficient to induce clear cellular differentiation towards a profibrotic lineage, i.e. both profibrotic mediators αSMA and CTGF [84,85] were not differently expressed between platforms.

In conclusion, an increased degree of anisotropy enhanced the potential of cells to remodel their surrounding matrix. This may explain the poor regenerative capacity of tenocytes in chronic tendinopathy and the observation that the structure of affected tendon tissue is never fully recovered [29,53–57].

Materials and methods

Cell extraction and culturing

Tendon-derived cells were isolated from tail tendon fascicles from C57BL/6 mice (permission granted under number ZH265/14, Kantonales Veterinäramt Zürich, “The role of cells and matrix mechanics in degeneration and regeneration of rodent tendon tissue”). Upon euthanization of the animal using carbon dioxide gas, the tail was cut and rinsed in 80% ethanol. The tip of the tail was clamped with a locking forceps and twisted to extract tail tendon fascicles. Fascicles were placed in PBS and the part of the tail in the locking forceps was cut off, leaving only the tendon tissue. The procedure was repeated to extract all fascicles from the tail after which fascicles were placed in a PBS-Collagenase IV solution (3 mg/mL, Thermo Scientific nr. 17,104–019) for 4 h at 37 degrees Celsius in a rotating chamber. The solution was centrifuged 5 min at 1100 rpm and the collagenase was aspirated. Cells and remnants of tendon fascicles were resuspended in growth medium

Please cite this article as: J. Foolen, et al., Tissue alignment enhances remodeling potential of tendon-derived cells - Lessons from a novel microtissue model of tendon scarri..., Matrix Biol (2017), http://dx.doi.org/10.1016/j.matbio.2017.06.002

(DMEM 6429, Sigma; 10% fetal bovine serum, Thermo Fisher Scientific; 1% penicillin/streptomycin, Sigma; 1% nonessential amino acids, Sigma) and cultured in collagen type I coated T75 flasks. All culture flasks were coated overnight with collagen type I (rat tail, Advanced Biomatrix nr. 5056) at 50 μg/mL in PBS (Sigma). After 2 days, cells were passaged (1:2) using trypsin (Thermo Fisher Scientific) and cultured for another 2 days (37 degrees Celsius, 5% CO_2). Subsequently, they were frozen and stored in growth medium containing 20% DMSO (Sigma). Before deployment into reconstituted collagen tissues, cells were passages once more (culturing them twice in 2D for 3 days), resulting in all tendon-derived cells to be used at passage 4 (in total after 10 days of culturing in 2D).

Model system

An adapted version of a previously designed model system [51,86,87] was used, able to engineer small-scale cell-populated fibrous tissues (Fig. 1). Cell-populated reconstituted collagen matrices were produced via anchorage around an array of silicone posts, resulting in constrained tissues in which alignment progressively decreased from strongly anisotropic to isotropic (Fig. 1), or from an initial setup of 10 Posts (unperturbed and isotropic) remodeling towards a 6 posts setup (perturbed and anisotropic) due to flipping the tissue over the perpendicular posts at day 2 after the start of culturing using a forceps (Fig. 6). Posts were mounted on rigid substrates, where deflection of posts upon tissue contraction was not observed. A gel mixture of growth medium, collagen type I (rat tail, Advanced Biomatrix nr. 5056) and 1 M NaOH, to neutralize the acidic collagen solution, was made with a final collagen concentration of 1.5 mg/mL. Tendon-derived cells were mixed with the gel at 5 million cells per mL gel. The cell-gel mixture was subsequently added to the system and left to gel for 45 min, after which warm growth medium was added to each well (4 mL). After 4 or 7 days of culturing, tissues were directly put in liquid nitrogen for RNA isolation, or tissues were fixed in 10% formalin solution (Sigma-Aldrich, HT5011) when anchored to the posts for 30 min for microscopy purposes.

Staining & microscopy

Top view phase contrast images of the tissues on the different setups, as presented in Figs. 1, 2, 4–6, were taken with an EVOS XL Core imaging system (Thermo Scientific).

For polarized light microscopy, fixed tissues were incubated for 2 h at room temperature in a Nuclear Fast Red solution (Sigma, 229,113; 0.5 g in 500 mL picric acid solution) and subsequently washed twice in acidified water (5 mL acetic acid in 1 L deionized water). Imaging was performed using a Leica (Leica DM5500 B inverted microscope) with a 10× objective (Leica HC PL FL 10×, 0.3 N.A.), connected to a digital camera (Leica DFC360 FX). Images were stitched together using Fiji.

For confocal laser scanning microscopy, fixed tissues were permeabilized for 30 min in 0.5% Triton-X in PBS. The following antibodies were used for specific staining of cellular proteins and cell nuclei: αSMA primary antibody ab5694 (1:100, Abcam) and FITC-labeled secondary antibody 711–095-152 (1:50, Jackson ImmunoResearch Laboratories); connexin43 primary antibody MAB3067 (1:100, Sigma-Aldrich) and Alexa Fluor 488-labeled secondary antibody A-21202 (1:50, ThermoFisher Scientific); actin cytoskeleton using Alexa Fluor 568 nm Phalloidin (1:100, ThermoFisher Scientific); and cell nuclei are stained with Hoechst (2 drops/mL, R37605, Molecular Probes). Staining of αSMA and connexin43 was never performed on the same tissue because of corresponding excitation wavelengths. *Z*-stack fluorescent images were taken with a confocal microscope (Leica SP5 CLSM). The pinhole of the photo-multiplier was set to the optimal width for the used 63×, 1.3 N.A. glycerol immersion lens (Zeiss HCX PL Apo, #506194). Excitation sources comprised of a 405 nm diode laser set at 20% power, a 488 nm argon laser set at 10% power and a 561 nm DPSS laser set at 10% power. Hybrid detectors accepted wavelength regions of 423–472 nm for Hoechst, 498-541 nm for FITC (αSMA or connexin43), or 571-640 nm for Alexa Fluor 568 nm phalloidin. Tissues, released from the posts, were visualized through the glass bottom of a petri dish. Presented images were taken beyond the tissue surface layer to ensure imaging of cells in a true 3D environment with 2× line averaging and measured 246x246μm each. No additional image processing was performed.

rtPCR

Pooled tissues were taken from liquid nitrogen storage and lysed directly in RLT buffer, containing 1% β-mercaptoethanol (Sigma). The RNeasy Plus Micro Kit protocol was followed to isolate RNA from the samples (Qiagen, 74,004). The quality and quantity of the RNA was measured for each sample taking 2 μL sample using an Epoch Microplate Spectrophotometer, loaded with a Take3 micro-volume plate (Biotek). Subsequently, complementary DNA (cDNA) was produced from the RNA solution, diluted to 20 ng/mL RNA in RNase-free water, with the High Capacity RNA-to-cDNA Kit (Applied Biosystems, 4,387,406).

Quantitative real-time PCR (qRT-PCR) was performed using TaqMan primers (ThermoFisher Scientific, Table 1). qRT-PCR reactions consisted of 2 μL cDNA sample, 2.5 μL RNase-free water, 0.5 μL primer, and 5 μL mastermix (TaqMan Universal Master Mix, Applied Biosystems, 4,304,437). Samples were amplified using a CFX96 RT-PCR Detection

Please cite this article as: J. Foolen, et al., Tissue alignment enhances remodeling potential of tendon-derived cells - Lessons from a novel microtissue model of tendon scarri..., Matrix Biol (2017), http://dx.doi.org/10.1016/j.matbio.2017.06.002

Table 1. TaqMan primers used in the current study (ThermoFisher Scientific).

Eukaryotic initiation factor 4a2	Eif4a2	Mm01730183_gH
Glyceraldehyde 3-phophate dehydrogenase	Gapdh	Mm00801666_g1
Ribosomal Protein (large subunit) 4	Rpl4	Mm0171353_g1
Ornithine decarboxylase antizyme	Oaz1	Mm01611061_g1
Ribosomal Protein (small subunit) 29	Rps29	Mm02342448_gH
Small ribosomal protein 14	Srp14	Mm00726104_s1
Scleraxis	Scx	Mm01205675_m1
Tenomodulin	Tnmd	Mm00491594_m1
Mohawk	Mkx	Mm00617017_m1
Collagen 1	Col1a1	Mm00801666_g1
Collagen 3	Col3a1	Mm01254476_m1
Matrix Metalloproteinase 1	MMP1	Mm00473485_m1
Matrix Metalloproteinase 2	MMP2	Mm00439498_m1
Matrix Metalloproteinase 3	MMP3	Mm00440295_m1
Matrix Metalloproteinase 9	MMP9	Mm00442991_m1
Matrix Metalloproteinase 13	MMP13	Mm00439491_m1
Matrix Metalloproteinase 14	MMP14	Mm00485054_m1
Tissue inhibitor of metalloproteinase 1	TIMP1	Mm01341361_m1
Tissue inhibitor of metalloproteinase 2	TIMP2	Mm00441825_m1
Alpha Smooth Muscle Actin	αSMA	Mm00725412_s1
Decorin	Dcn	Mm00514535_m1
Connexin 26	Cx26/Gjb2	Mm00433643_s1
Connexin 32	Cx32/Gjb1	Mm01950058_s1
Connexin 43	Cx43/Gja1	Mm01179639_s1

System (Biorad) under the following PCR cycling conditions: 50 °C for 2 min, 95 °C for 10 min, 40 cycles of denaturation at 95 °C for 15 s, annealing and extension at 60 °C for 5 s. Quantification was done using the comparative $2^{-\Delta\Delta CT}$ method with the eukaryotic initiation factor-4A2 (Eif4a2) as housekeeping gene, since that was shown to be the most stable of tested housekeeping genes (Supplementary Fig. S1, values were normalized against the average value from all samples of the gene tested). Results are presented as relative gene expression levels normalized to tissues that originated from the 2 posts setup ('unscarred' tendon), which thus have the value 1 and lack a standard deviation. All reactions were performed in technical duplicates or triplicates.

Numerical model

A previously established computational framework [50–52] was utilized to predict the local actin stress fiber alignment throughout the whole tissue in each of the setups. The posts in each of the setups were modeled as incompressible Neo-Hookean materials with a Young's modulus of 0.27 MPa. The tissue was modeled as a mixture of actin stress fibers, collagen fibers, and isotropic cell and tissue constituents, where stress fibers and collagen fibers were both modeled as angular distributions of fibers. The volume fractions of stress fibers in all directions were subject to remodeling, whereas the collagen volume fractions were equal in all directions (no remodeling). Remodeling of the actin stress fibers was hypothesized to depend on the active stress exerted by the stress fibers, where the stress fiber stress was modeled as a function of the strain and strain rate in the tissue [51]. In addition, contraction of the collagen fibers, induced by the contractile forces of the stress fibers, was included as a mechanism for tissue compaction [52]. The following order parameter was used to quantify the strength and main orientation of the stress fiber distribution at each location:

$$O_{sf} = \int_{-\pi/2}^{\pi/2} \frac{\varphi_{sf}(\gamma)}{N(\varphi_a - \varphi_m)} \cos(2\gamma) d\gamma$$

with $\varphi_{sf}(\gamma)$ the stress fiber volume fraction at angle γ, N the number of fiber directions, φ_a the total amount of actin, and φ_m the fraction of actin that had not polymerized into stress fibers. To quantify the strength of alignment only, the stress fiber distribution at each location in the tissue was fitted with a periodic version of the normal probability distribution:

$$\tilde{\varphi}_{sf} = A \ \exp\left(\frac{\cos[2(\gamma-\alpha)+1]}{\beta}\right)$$

where α is the main angle of the fiber distribution, and β is a measure for the fiber dispersity. Subsequently, a measure for the mean cellular alignment strength of the complete tissue (Mean Strength A) was obtained as:

$$S_A = \frac{1}{V}\int_V \frac{\tilde{\varphi}_{\text{sf,peak}}}{\beta} dV$$

with $\tilde{\varphi}_{sf,peak}$ the peak of the fitted distribution, and V the volume of the tissue. Finally, to explore the consequences of a nonlinear dependence of gene

Please cite this article as: J. Foolen, et al., Tissue alignment enhances remodeling potential of tendon-derived cells - Lessons from a novel microtissue model of tendon scarri..., Matrix Biol (2017), http://dx.doi.org/10.1016/j.matbio.2017.06.002

expression on local cell alignment, the following index was proposed (Mean Strength B):

$$S_B = \frac{1}{V}\int_V \exp\frac{\tilde{\varphi}_{sf,peak}}{\beta}\, dV$$

Statistics

One-way ANOVA was performed on rtPCR data (for all experiments, $n = 3$), as presented in Fig. 3, to detect a significant difference between the different post setups (2–12 posts). *P*-values below 0.05 were considered to indicate a significant change in gene expression level for the different post setups. Post hoc tests were not performed because of the normalization procedure against the 2 post setup (values always equal 1 without a standard deviation).

Supplementary data to this article can be found online at http://dx.doi.org/10.1016/j.matbio.2017.06.002.

Authorship contributions

J.G.S. supervised the project. J.G.S. and J.F. developed the project idea and contributed to the study design. J.F., S.L.W. & S.L. performed the experiments. J.F., J.G.S and S.L. analyzed the data and J.F. and S.L. prepared the figures. All authors contributed to writing and editing the paper.

Acknowledgements

The research leading to these results has received funding from the European Union Seventh Framework Programme (FP7/2007–2013) under grant agreement no. PIEF-GA-2013-628585 (Jasper Foolen). We gratefully acknowledge Patrick Jaeger for drawing the illustrative model system images.

Received 30 March 2017;
Received in revised form 29 May 2017;
Accepted 4 June 2017
Available online xxxx

References

[1] A. McCormick, J. Charlton, D. Fleming, Assessing health needs in primary care. Morbidity study from general practice provides another source of information, BMJ 310 (1995) 1534.

[2] K. Spanoudes, D. Gaspar, A. Pandit, D.I. Zeugolis, The biophysical, biochemical, and biological toolbox for tenogenic phenotype maintenance in vitro, Trends Biotechnol. 32 (2014) 474–482.

[3] H.B. Sun, N. Andarawis-Puri, Y. Li, D.T. Fung, J.Y. Lee, V.M. Wang, J. Basta-Pljakic, D.J. Leong, J.B. Sereysky, S.J. Ros, R.A. Klug, J. Braman, M.B. Schaffler, K.J. Jepsen, E.L. Flatow, Cycle-dependent matrix remodeling gene expression response in fatigue-loaded rat patellar tendons, J. Orthop. Res. 28 (2010) 1380–1386.

[4] T.A. Jarvinen, P. Kannus, N. Maffulli, K.M. Khan, Achilles tendon disorders: etiology and epidemiology, Foot Ankle Clin. 10 (2005) 255–266.

[5] T.L. Willett, R.S. Labow, N.C. Avery, J.M. Lee, Increased proteolysis of collagen in an in vitro tensile overload tendon model, Ann. Biomed. Eng. 35 (2007) 1961–1972.

[6] L.J. Soslowsky, S. Thomopoulos, S. Tun, C.L. Flanagan, C.C. Keefer, J. Mastaw, J.E. Carpenter, Neer Award 1999. Overuse activity injures the supraspinatus tendon in an animal model: a histologic and biomechanical study, J. Shoulder Elb. Surg. 9 (2000) 79–84.

[7] J.D. Rees, A.M. Wilson, R.L. Wolman, Current concepts in the management of tendon disorders, Rheumatology (Oxford) 45 (2006) 508–521.

[8] G. Riley, Tendinopathy–from basic science to treatment, Nat. Clin. Pract. Rheumatol. 4 (2008) 82–89.

[9] Y. Haglund-Akerlind, E. Eriksson, Range of motion, muscle torque and training habits in runners with and without Achilles tendon problems, Knee Surg. Sports Traumatol. Arthrosc. 1 (1993) 195–199.

[10] R.K. Smith, H.L. Birch, S. Goodman, D. Heinegard, A.E. Goodship, The influence of ageing and exercise on tendon growth and degeneration–hypotheses for the initiation and prevention of strain-induced tendinopathies, Comp. Biochem. Physiol. A Mol. Integr. Physiol. 133 (2002) 1039–1050.

[11] D. Kader, A. Saxena, T. Movin, N. Maffulli, Achilles tendinopathy: some aspects of basic science and clinical management, Br. J. Sports Med. 36 (2002) 239–249.

[12] B.R. Bach Jr., M.E. Levy, J. Bojchuk, S. Tradonsky, C.A. Bush-Joseph, N.H. Khan, Single-incision endoscopic anterior cruciate ligament reconstruction using patellar tendon autograft. Minimum two-year follow-up evaluation, Am. J. Sports Med. 26 (1998) 30–40.

[13] B.R. Bach Jr., S. Tradonsky, J. Bojchuk, M.E. Levy, C.A. Bush-Joseph, N.H. Khan, Arthroscopically assisted anterior cruciate ligament reconstruction using patellar tendon autograft. Five- to nine-year follow-up evaluation, Am. J. Sports Med. 26 (1998) 20–29.

[14] S.F. Badylak, R. Tullius, K. Kokini, K.D. Shelbourne, T. Klootwyk, S.L. Voytik, M.R. Kraine, C. Simmons, The use of xenogeneic small intestinal submucosa as a biomaterial for Achilles tendon repair in a dog model, J. Biomed. Mater. Res. 29 (1995) 977–985.

[15] H.H. Lu, J. Jiang, Interface tissue engineering and the formulation of multiple-tissue systems, Adv. Biochem. Eng. Biotechnol. 102 (2006) 91–111.

[16] W. Maletius, J. Gillquist, Long-term results of anterior cruciate ligament reconstruction with a Dacron prosthesis. The frequency of osteoarthritis after seven to eleven years, Am. J. Sports Med. 25 (1997) 288–293.

[17] L.M. Galatz, C.M. Ball, S.A. Teefey, W.D. Middleton, K. Yamaguchi, The outcome and repair integrity of completely arthroscopically repaired large and massive rotator cuff tears, J. Bone Joint Surg. Am. 86-A (2004) 219–224.

[18] J. Bishop, S. Klepps, I.K. Lo, J. Bird, J.N. Gladstone, E.L. Flatow, Cuff integrity after arthroscopic versus open rotator

cuff repair: a prospective study, J. Shoulder Elb. Surg. 15 (2006) 290–299.
[19] T. Pufe, W. Petersen, B. Kurz, M. Tsokos, B. Tillmann, R. Mentlein, Mechanical factors influence the expression of endostatin—an inhibitor of angiogenesis—in tendons, J. Orthop. Res. 21 (2003) 610–616.
[20] T. Pufe, W.J. Petersen, R. Mentlein, B.N. Tillmann, The role of vasculature and angiogenesis for the pathogenesis of degenerative tendons disease, Scand. J. Med. Sci. Sports 15 (2005) 211–222.
[21] M.D. McElvany, E. McGoldrick, A.O. Gee, M.B. Neradilek, F.A. Matsen III, Rotator cuff repair: published evidence on factors associated with repair integrity and clinical outcome, Am. J. Sports Med. 43 (2015) 491–500.
[22] C. Frank, D. McDonald, D. Bray, R. Bray, R. Rangayyan, D. Chimich, N. Shrive, Collagen fibril diameters in the healing adult rabbit medial collateral ligament, Connect. Tissue Res. 27 (1992) 251–263.
[23] G. Pelled, J.G. Snedeker, A. Ben-Arav, S. Rigozzi, Y. Zilberman, N. Kimelman-Bleich, Z. Gazit, R. Muller, D. Gazit, Smad8/BMP2-engineered mesenchymal stem cells induce accelerated recovery of the biomechanical properties of the Achilles tendon, J. Orthop. Res. 30 (2012) 1932–1939.
[24] R.C. Marqueti, N.A. Parizotto, R.S. Chriguer, S.E. Perez, H.S. Selistre-de-Araujo, Androgenic-anabolic steroids associated with mechanical loading inhibit matrix metallopeptidase activity and affect the remodeling of the achilles tendon in rats, Am. J. Sports Med. 34 (2006) 1274–1280.
[25] S.J. Kew, J.H. Gwynne, D. Enea, M. Abu-Rub, A. Pandit, D. Zeugolis, R.A. Brooks, N. Rushton, S.M. Best, R.E. Cameron, Regeneration and repair of tendon and ligament tissue using collagen fibre biomaterials, Acta Biomater. 7 (2011) 3237–3247.
[26] E.T. Ricchetti, A. Aurora, J.P. Iannotti, K.A. Derwin, Scaffold devices for rotator cuff repair, J. Shoulder Elb. Surg. 21 (2012) 251–265.
[27] U.G. Longo, A. Lamberti, N. Maffulli, V. Denaro, Tendon augmentation grafts: a systematic review, Br. Med. Bull. 94 (2010) 165–188.
[28] J.A. Cadby, F. David, C. van de Lest, G. Bosch, P.R. van Weeren, J.G. Snedeker, H.T. van Schie, Further characterisation of an experimental model of tendinopathy in the horse, Equine Vet. J. 45 (2013) 642–648.
[29] K. Nagasawa, M. Noguchi, K. Ikoma, T. Kubo, Static and dynamic biomechanical properties of the regenerating rabbit Achilles tendon, Clin. Biomech. (Bristol, Avon) 23 (2008) 832–838.
[30] S.I. Docking, J. Cook, Pathological tendons maintain sufficient aligned fibrillar structure on ultrasound tissue characterization (UTC), Scand. J. Med. Sci. Sports 26 (2016) 675–683.
[31] W.R. Su, H.H. Chen, Z.P. Luo, Effect of cyclic stretching on the tensile properties of patellar tendon and medial collateral ligament in rat, Clin. Biomech. (Bristol, Avon) 23 (2008) 911–917.
[32] C.L. Mendias, J.P. Gumucio, K.I. Bakhurin, E.B. Lynch, S.V. Brooks, Physiological loading of tendons induces scleraxis expression in epitenon fibroblasts, J. Orthop. Res. 30 (2012) 606–612.
[33] C.L. Mendias, J.P. Gumucio, Lynch EB (2012) mechanical loading and TGF-beta change the expression of multiple miRNAs in tendon fibroblasts, J. Appl. Physiol. 113 (1985) 56–62.
[34] J.Z. Paxton, P. Hagerty, J.J. Andrick, K. Baar, Optimizing an intermittent stretch paradigm using ERK1/2 phosphorylation results in increased collagen synthesis in engineered ligaments, Tissue Eng. Part A 18 (2012) 277–284.
[35] N. Juncosa-Melvin, K.S. Matlin, R.W. Holdcraft, V.S. Nirmalanandhan, D.L. Butler, Mechanical stimulation increases collagen type I and collagen type III gene expression of stem cell-collagen sponge constructs for patellar tendon repair, Tissue Eng. 13 (2007) 1219–1226.
[36] J. Qi, L. Chi, D. Bynum, Banes AJ (2011) gap junctions in IL-1beta-mediated cell survival response to strain, J. Appl. Physiol. 110 (1985) 1425–1431.
[37] B.T. Drew, T.O. Smith, C. Littlewood, B. Sturrock, Do structural changes (e.g., collagen/matrix) explain the response to therapeutic exercises in tendinopathy: a systematic review, Br. J. Sports Med. 48 (2014) 966–972.
[38] J.L. Cook, E. Rio, C.R. Purdam, S.I. Docking, Revisiting the continuum model of tendon pathology: what is its merit in clinical practice and research? Br. J. Sports Med. 50 (2016) 1187–1191.
[39] C.S. Chen, M. Mrksich, S. Huang, G.M. Whitesides, D.E. Ingber, Geometric control of cell life and death, Science 276 (1997) 1425–1428.
[40] Y. Yang, N.K. Relan, D.A. Przywara, L. Schuger, Embryonic mesenchymal cells share the potential for smooth muscle differentiation: myogenesis is controlled by the cell's shape, Development 126 (1999) 3027–3033.
[41] K.A. Kilian, B. Bugarija, B.T. Lahn, M. Mrksich, Geometric cues for directing the differentiation of mesenchymal stem cells, Proc. Natl. Acad. Sci. U. S. A. 107 (2010) 4872–4877.
[42] C.L. Gilchrist, D.S. Ruch, D. Little, F. Guilak, Micro-scale and meso-scale architectural cues cooperate and compete to direct aligned tissue formation, Biomaterials 35 (2014) 10015–10024.
[43] J. Zhu, J. Li, B. Wang, W.J. Zhang, G. Zhou, Y. Cao, W. Liu, The regulation of phenotype of cultured tenocytes by microgrooved surface structure, Biomaterials 31 (2010) 6952–6958.
[44] Z. Yin, X. Chen, J.L. Chen, W.L. Shen, T.M. Hieu Nguyen, L. Gao, H.W. Ouyang, The regulation of tendon stem cell differentiation by the alignment of nanofibers, Biomaterials 31 (2010) 2163–2175.
[45] Z. Yin, X. Chen, H.X. Song, J.J. Hu, Q.M. Tang, T. Zhu, W.L. Shen, J.L. Chen, H. Liu, B.C. Heng, H.W. Ouyang, Electrospun scaffolds for multiple tissues regeneration in vivo through topography dependent induction of lineage specific differentiation, Biomaterials 44 (2015) 173–185.
[46] C.M. McNeilly, A.J. Banes, M. Benjamin, J.R. Ralphs, Tendon cells in vivo form a three dimensional network of cell processes linked by gap junctions, J. Anat. 189 (Pt 3) (1996) 593–600.
[47] E. Maeda, S. Ye, W. Wang, D.L. Bader, M.M. Knight, D.A. Lee, Gap junction permeability between tenocytes within tendon fascicles is suppressed by tensile loading, Biomech. Model. Mechanobiol. 11 (2012) 439–447.
[48] J.A. Gordon, B.R. Freedman, A. Zuskov, R.V. Iozzo, D.E. Birk, L.J. Soslowsky, Achilles tendons from decorin- and biglycan-null mouse models have inferior mechanical and structural properties predicted by an image-based empirical damage model, J. Biomech. 48 (2015) 2110–2115.
[49] M.L. Bayer, P. Schjerling, A. Herchenhan, C. Zeltz, K.M. Heinemeier, L. Christensen, M. Krogsgaard, D. Gullberg, M. Kjaer, Release of tensile strain on engineered human tendon tissue disturbs cell adhesions, changes matrix architecture, and induces an inflammatory phenotype, PLoS One 9 (2014) e86078.
[50] C. Obbink-Huizer, J. Foolen, C.W. Oomens, M. Borochin, C.S. Chen, C.V. Bouten, F.P. Baaijens, Computational and

Please cite this article as: J. Foolen, et al., Tissue alignment enhances remodeling potential of tendon-derived cells - Lessons from a novel microtissue model of tendon scarri..., Matrix Biol (2017), http://dx.doi.org/10.1016/j.matbio.2017.06.002

experimental investigation of local stress fiber orientation in uniaxially and biaxially constrained microtissues, Biomech. Model. Mechanobiol. 13 (2014) 1053–1063.
[51] C. Obbink-Huizer, C.W. Oomens, S. Loerakker, J. Foolen, C.V. Bouten, F.P. Baaijens, Computational model predicts cell orientation in response to a range of mechanical stimuli, Biomech. Model. Mechanobiol. 13 (2014) 227–236.
[52] S. Loerakker, C. Obbink-Huizer, F.P. Baaijens, A physically motivated constitutive model for cell-mediated compaction and collagen remodeling in soft tissues, Biomech. Model. Mechanobiol. 13 (2014) 985–1001.
[53] A.J. Lomas, C.N. Ryan, A. Sorushanova, N. Shologu, A.I. Sideri, V. Tsioli, G.C. Fthenakis, A. Tzora, I. Skoufos, L.R. Quinlan, G. O'Laighin, A.M. Mullen, J.L. Kelly, S. Kearns, M. Biggs, A. Pandit, D.I. Zeugolis, The past, present and future in scaffold-based tendon treatments, Adv. Drug Deliv. Rev. 84 (2015) 257–277.
[54] P. Sharma, N. Maffulli, Biology of tendon injury: healing, modeling and remodeling, J. Musculoskelet. Neuronal Interact. 6 (2006) 181–190.
[55] P.B. Voleti, M.R. Buckley, L.J. Soslowsky, Tendon healing: repair and regeneration, Annu. Rev. Biomed. Eng. 14 (2012) 47–71.
[56] J.E. Carpenter, S. Thomopoulos, C.L. Flanagan, C.M. DeBano, L.J. Soslowsky, Rotator cuff defect healing: a biomechanical and histologic analysis in an animal model, J. Shoulder Elb. Surg. 7 (1998) 599–605.
[57] R.P. Janssen, S.U. Scheffler, Intra-articular remodelling of hamstring tendon grafts after anterior cruciate ligament reconstruction, Knee Surg. Sports Traumatol. Arthrosc. 22 (2014) 2102–2108.
[58] I.F. Williams, A. Heaton, K.G. McCullagh, Cell morphology and collagen types in equine tendon scar, Res. Vet. Sci. 28 (1980) 302–310.
[59] N. Maffulli, S.W. Ewen, S.W. Waterston, J. Reaper, V. Barrass, Tenocytes from ruptured and tendinopathic achilles tendons produce greater quantities of type III collagen than tenocytes from normal achilles tendons. An in vitro model of human tendon healing, Am. J. Sports Med. 28 (2000) 499–505.
[60] A. Pajala, J. Melkko, J. Leppilahti, P. Ohtonen, Y. Soini, J. Risteli, Tenascin-C and type I and III collagen expression in total Achilles tendon rupture. An immunohistochemical study, Histol. Histopathol. 24 (2009) 1207–1211.
[61] J.M. Archambault, S.A. Jelinsky, S.P. Lake, A.A. Hill, D.L. Glaser, L.J. Soslowsky, Rat supraspinatus tendon expresses cartilage markers with overuse, J. Orthop. Res. 25 (2007) 617–624.
[62] S.M. Perry, S.E. McIlhenny, M.C. Hoffman, L.J. Soslowsky, Inflammatory and angiogenic mRNA levels are altered in a supraspinatus tendon overuse animal model, J. Shoulder Elb. Surg. 14 (2005) 79S–83S.
[63] M. Attia, A. Scott, A. Duchesnay, G. Carpentier, L.J. Soslowsky, M.B. Huynh, T.H. Van Kuppevelt, C. Gossard, J. Courty, M.C. Tassoni, I. Martelly, Alterations of overused supraspinatus tendon: a possible role of glycosaminoglycans and HARP/pleiotrophin in early tendon pathology, J. Orthop. Res. 30 (2012) 61–71.
[64] M. Magra, N. Maffulli, Matrix metalloproteases: a role in overuse tendinopathies, Br. J. Sports Med. 39 (2005) 789–791.
[65] M. Leung, A. Cooper, S. Jana, C.T. Tsao, T.A. Petrie, M. Zhang, Nanofiber-based in vitro system for high myogenic differentiation of human embryonic stem cells, Biomacromolecules 14 (2013) 4207–4216.
[66] J. Malmstrom, H. Lindberg, C. Lindberg, C. Bratt, E. Wieslander, E.L. Delander, B. Sarnstrand, J.S. Burns, P. Mose-Larsen, S. Fey, G. Marko-Varga, Transforming growth factor-beta 1 specifically induce proteins involved in the myofibroblast contractile apparatus, Mol. Cell. Proteomics 3 (2004) 466–477.
[67] B.C. Willis, Z. Borok, TGF-beta-induced EMT: mechanisms and implications for fibrotic lung disease, Am. J. Physiol. Lung Cell. Mol. Physiol. 293 (2007) L525–L534.
[68] N. Andarawis-Puri, E.L. Flatow, L.J. Soslowsky, Tendon basic science: development, repair, regeneration, and healing, J. Orthop. Res. 33 (2015) 780–784.
[69] M. Abate, K.G. Silbernagel, C. Siljeholm, I.A. Di, A.D. De, V. Salini, S. Werner, R. Paganelli, Pathogenesis of tendinopathies: inflammation or degeneration? Arthritis Res. Ther. 11 (2009).
[70] G.P. Riley, V. Curry, J. DeGroot, E.B. van, N. Verzijl, B.L. Hazleman, R.A. Bank, Matrix metalloproteinase activities and their relationship with collagen remodelling in tendon pathology, Matrix Biol. 21 (2002) 185–195.
[71] A. DelBuono, F. Oliva, U.G. Longo, S.A. Rodeo, J. Orchard, V. Denaro, N. Maffulli, Metalloproteases and rotator cuff disease, J. Shoulder Elb. Surg. 21 (2012) 200–208.
[72] B. Pasternak, M. Fellenius, P. Aspenberg, Doxycycline impairs tendon repair in rats, Acta Orthop. Belg. 72 (2006) 756–760.
[73] A. Castagna, E. Cesari, A. Gigante, M. Conti, R. Garofalo, Metalloproteases and their inhibitors are altered in both torn and intact rotator cuff tendons, Musculoskelet. Surg. 97 (Suppl. 1) (2013) 39–47.
[74] C.T. Thorpe, S. Chaudhry, I.I. Lei, A. Varone, G.P. Riley, H.L. Birch, P.D. Clegg, H.R. Screen, Tendon overload results in alterations in cell shape and increased markers of inflammation and matrix degradation, Scand. J. Med. Sci. Sports 25 (2015) e381–e391.
[75] K. Gardner, S.P. Arnoczky, O. Caballero, M. Lavagnino, The effect of stress-deprivation and cyclic loading on the TIMP/MMP ratio in tendon cells: an in vitro experimental study, Disabil. Rehabil. 30 (2008) 1523–1529.
[76] M. Nomura, Y. Hosaka, Y. Kasashima, H. Ueda, K. Takehana, A. Kuwano, K. Arai, Active expression of matrix metalloproteinase-13 mRNA in the granulation tissue of equine superficial digital flexor tendinitis, J. Vet. Med. Sci. 69 (2007) 637–639.
[77] H.B. Sun, Y. Li, D.T. Fung, R.J. Majeska, M.B. Schaffler, E.L. Flatow, Coordinate regulation of IL-1beta and MMP-13 in rat tendons following subrupture fatigue damage, Clin. Orthop. Relat. Res. 466 (2008) 1555–1561.
[78] M. Kjaer, Role of extracellular matrix in adaptation of tendon and skeletal muscle to mechanical loading, Physiol. Rev. 84 (2004) 649–698.
[79] R.L. Stanley, R.A. Fleck, D.L. Becker, A.E. Goodship, J.R. Ralphs, J.C. Patterson-Kane, Gap junction protein expression and cellularity: comparison of immature and adult equine digital tendons, J. Anat. 211 (2007) 325–334.
[80] Y. Liu, H.S. Ramanath, D.A. Wang, Tendon tissue engineering using scaffold enhancing strategies, Trends Biotechnol. 26 (2008) 201–209.
[81] W.Y. Tong, W. Shen, C.W. Yeung, Y. Zhao, S.H. Cheng, P.K. Chu, D. Chan, G.C. Chan, K.M. Cheung, K.W. Yeung, Y.W. Lam, Functional replication of the tendon tissue microenvironment by a bioimprinted substrate and the support of tenocytic differentiation of mesenchymal stem cells, Biomaterials 33 (2012) 7686–7698.
[82] S.R. Caliari, B.A. Harley, Structural and biochemical modification of a collagen scaffold to selectively enhance MSC tenogenic, chondrogenic, and osteogenic differentiation, Adv. Healthc. Mater. 3 (2014) 1086–1096.

Please cite this article as: J. Foolen, et al., Tissue alignment enhances remodeling potential of tendon-derived cells - Lessons from a novel microtissue model of tendon scarri..., Matrix Biol (2017), http://dx.doi.org/10.1016/j.matbio.2017.06.002

[83] V. Kishore, W. Bullock, X. Sun, W.S. Van Dyke, O. Akkus, Tenogenic differentiation of human MSCs induced by the topography of electrochemically aligned collagen threads, Biomaterials 33 (2012) 2137–2144.
[84] W. Morita, S.J. Snelling, S.G. Dakin, A.J. Carr, Profibrotic mediators in tendon disease: a systematic review, Arthritis Res. Ther. 18 (2016) 269.
[85] M.E. Berglund, K.A. Hildebrand, M. Zhang, D.A. Hart, M.E. Wiig, Neuropeptide, mast cell, and myofibroblast expression after rabbit deep flexor tendon repair, J. Hand. Surg. [Am.] 35 (2010) 1842–1849.
[86] J. Foolen, M.W. Janssen-van den Broek, F.P. Baaijens, Synergy between rho signaling and matrix density in cyclic stretch-induced stress fiber organization, Acta Biomater. 10 (2014) 1876–1885.
[87] J. Foolen, V.S. Deshpande, F.M. Kanters, F.P. Baaijens, The influence of matrix integrity on stress-fiber remodeling in 3D, Biomaterials 33 (2012) 7508–7518.

Please cite this article as: J. Foolen, et al., Tissue alignment enhances remodeling potential of tendon-derived cells - Lessons from a novel microtissue model of tendon scarri..., Matrix Biol (2017), http://dx.doi.org/10.1016/j.matbio.2017.06.002